SUPPORTING INFORMATION

Mechanism of Action of the Boron-Dependent Antibiotic Entails Synergistic Binding

Shao-Lun Chiou[1], Jacky Lin[1], Jiayuan Miao[2], Yi-Hsuan Tsai[1], Ching-Wen Chiu[1], Yu-Shan Lin[2], John Chu[1,3]*

[1] Department of Chemistry, National Taiwan University, No. 1 Sec. 4, Roosevelt Rd., Taipei 10617, Taiwan. [2] Department of Chemistry, Tufts University, 62 Talbot Avenue, Medford, MA 02155, USA. [3] Center for Emerging Material and Advanced Devices, National Taiwan University, No. 1 Sec. 4, Roosevelt Rd., Taipei 10617, Taiwan.

* Correspondence: johnchu@ntu.edu.tw

Table of Contents **Page**

Chemicals, buffers, and sample preparation

Phenylboronic acid (PBA) and 4-fluoro-phenylboronic acid (FPBA) were purchased from BLDpharm. Lysogeny broth (LB) and HEPES were purchased from BioShop Canada Inc. Other chemicals were purchased from Merck, ThermoFisher Scientific, J.T.Baker, and Uni-Onward Corp. All chemicals are of ACS grade (or higher) and used as is. Isothermal calorimetry measurements were performed in 20 mM Na-HEPES, 150 mM NaCl at pH 7.4. All solutions, including both the titrant and the analyte, were prepared in this buffer. LspC analogues **S1** and **B1** were prepared according to previously reported methods.[1] These peptides were prepared as 5 mM buffered stock solutions and stored at –80° C.

Isothermal titration calorimetry (ITC) data acquisition

Affinity ITC LV (TA instrument) was used for all ITC experiments, wherein the cell contained 200 μL of sample, the temperature was fixed at 25 °C, heat acquisition mode was set to "small", and stirring was set to 80 rpm. All experiments were performed in triplicates, wherein one representative trace is shown in the main text and the rest in Figure S1 to S8. Background titrations were performed in duplicates.

S1 experiments. S1 was prepared as either a 50 μM or 500 μM solution by diluting the 5 mM stock into the buffer described above. In the **S1**-calcium experiment, $CaCl_2$ (5 mM) was titrated into **S1** (50 μM, 200 μL) in the cell. In the **S1**-C10P experiment, C10P (5 mM) was titrated into **S1** (500 μM, 200 μL) in the cell. The **S1**-C10P interaction was measured in the presence, and then in the absence of $CaCl_2$ (5 mM). The first injection was 0.4 μL, which was followed by eighteen injections of 2 μL of the titrant with 180-second intervals between each injection.

B1 experiments. B1 was prepared as a 50 μM solution by diluting the 5 mM **B1** stock into the buffer described above. In the **B1**/PBA-C10P experiment, C10P (0.5 mM) was titrated into a premixed solution of 50 μM of **B1** and 250 μM of PBA in the cell. The interaction was measured in the presence, and then in the absence of $CaCl_2$ (5 mM). Titration settings were the same as the **S1** experiments,

except for an even longer waiting period between injections (500 seconds). In the **B1**-PBA experiment, PBA (1.1 mM) was titrated into **B1** (50 μM, 200 μL) in the cell. All experiments were conducted in triplicate, while those without significant interactions and control experiments were performed in duplicate.

ITC data analysis

The calorimetric data was analyzed using NanoAnalyze. The appropriate background titration trace was first subtracted from each dataset prior to data analysis. For example, C10P titration into buffer was subtracted from the **S1**-C10P experiment; PBA titration into buffer was subtracted from the **B1**-PBA experiment, etc. The first datapoint in an ITC experiment is typically an outlier and excluded from data analysis. We noticed that few of our experiments (will be specifically marked in the following text) show a few more outlier datapoints due to peptide aggregation in the absence of the C10P substrate. These datapoints were also excluded from data analysis and are indicated in the figure legend. The built-in "Independent" model in NanoAnalyze was used for curve fitting iterated 1,000 times and reported the 95% confidence interval. Thermodynamic parameters reported in this manuscript were the averages and standard deviations of triplicate experiments.

Minimum inhibitory concentration determination

A single bacterial colony (*Staphylococcus aureus subsp. aureus*, ATCC 29213) on an LB agar plate was inoculated into LB medium (Bioshop®) and grown overnight at 37° C to stationary phase. The resulting culture was diluted 5,000-fold and used as the inoculum to setup the MIC assay. **B1** was added to the growth medium to generate the working solution (128 μg/mL), which was used to generate a 50 μL per well two-fold dilution series across a 96-well microtiter plate from well 1 to 10. The last two wells were reserved for positive (no peptide) and negative (no bacteria) controls. Bacterial inoculum was then added to each well (50 μL), so that each well contained a total of 100 μL of solution, wherein the final peptide concentrations ranged from 64 to 0.125 μg/mL. The microtiter

plate was incubated statically at 37° C prior to readout. To determine whether our peptide depends on FPBA to suppress bacterial growth, FPBA was premixed in the growth medium at the appropriate concentration and used as the diluent to prepare the dilution series.

Nuclear magnetic resonance (NMR) experiments

NMR experiments were conducted on a Bruker AVIII 400 (400 MHz) spectrometer. Chemical shifts of ^{19}F (δ) are relative to $CFCl_3$. The **B1** stock solution (5 mM in buffer) was diluted by D_2O to generate a working sample with 10% (v/v) of D_2O. This sample underwent 128 scans. Following the addition of one equivalent of FPBA, the sample was incubated at room temperature for 1 hour before it was scanned. Then, more FPBA was added to reach a final stoichiometric ratio of 5:1 (FPBA/**B1**). This sample was scanned one hour and one week after preparation and saw no change in ^{19}F signal. ^{19}F NMR spectra of hydrofluoric acid (HF), trifluoroacetic acid (TFA), FPBA, and a solution of glucose (1 M) in saturated FPBA were also acquired.

Detection limit of B1 boronic ester formation

Under our experimental conditions and based on the performance of our NMR spectrometer, the detection limit of a ^{19}F species is approximately 100 μM. In other words, when no **B1**/FPBA binary complex can be detected based on ^{19}F NMR in a solution containing **B1** and FPBA, no more than 100 μM of this species is present, *i.e.*, [**B1**/FPBA] < 100 μM. Knowing that $[\mathbf{B1}]_o$ = 4.5 mM and $[FPBA]_o$ = 5 mM (the amount of **B1** and FPBA at the start of the experiment), the lower bound of the dissociation constant of this equilibrium can be estimated:

$$K_d > \frac{[\boldsymbol{B1}][FPBA]}{[\boldsymbol{B1}/FPBA]} = \frac{4.4 \times 4.9}{0.1} = 0.216\ M;\ K_a < 4.64\ M^{-1}$$

We thus concluded that **B1**/FPBA binary complex formation is extremely weak, if present at all.

Timescale of boronic ester formation

To estimate the timescale necessary to reach equilibrium, we surveyed the literature and identified several boronic acid / diol reactions that proceeds slowly. As one of the most extreme cases, the $k_{forward}$ and $k_{reverse}$ of the PBA and cis-1,2-cyclopentanediol condensation / hydrolysis equilibrium are 0.0216 $M^{-1}s^{-1}$ and 0.0014 s^{-1}, respectively.[7] A simulation with 1 ms steps was performed using these rate constants. The iteration loop was terminated when the reaction quotient (Q) and the equilibrium constant (K) differ by no more than 1% (Q/K > 0.99), at which point the reaction was deemed complete (equilibrated). The initial concentration of the boronic acid and the diol ligand were set based on our ITC experiment condition, wherein [PBA] = 12.5 μM and [**B1**] = 50 μM. Under these conditions, the boronic ester formation / hydrolysis takes 3,287 s (54.8 min) to reach equilibrium. To ensure that our experiment conditions would be able to accommodate such a slow reaction, we ran an ITC experiment with one-hour intervals in between titrations and saw no detectable release of heat. Furthermore, samples were incubated at room temperature for at least one hour prior to ^{19}F NMR experiments. The **B1**/FPBA mixture was scanned one week after preparation and saw no change in ^{19}F signal.

Molecular dynamics (MD) simulations

Initial structure preparation. The initial structure of the **B1**/PBA/C10P ternary complex was reported previously.[1,2] Since our ITC results showed Ca(II) did not influence the stability of this complex, Ca(II) was excluded from the current simulations. The three oxygen–boron bonds (C10P (phosphate)–PBA, Ser7–PBA, and Ser1–PBA) were removed one at a time using the Maestro software from Schrödinger,[3] generating three complexes in which the boron is sp^2 hybridized with an empty p orbital and adopts a trigonal planar geometry. In the initial structures, all amide bonds were in the *trans* configuration. The topology file for each complex was generated using the Schrödinger utility ffld_server and converted to GROMACS format using the ffconv.py script.[4] Extra improper dihedrals related to the H, N, C, O atoms of the peptide bonds were applied to suppress the formation of cis

bonds. All MD simulations in this study were performed using GROMACS 2018.8[5] with the OPLS-2005 force field[6] and the TIP4P water model.[7]

Solvation and equilibration for explicit-solvent simulations. The following protocol was the same as our previous work.[1] Briefly, each initial structure was first energy minimized in vacuum using the steepest descent algorithm, and then solvated using a pre-equilibrated box of water molecules, with the minimum distance of 1.0 nm between the complex and the box walls. Sodium ions (Na^+) were added to neutralize the system. The energy of each solvated system was then minimized using the steepest descent algorithm, followed by a four-step equilibration process. Five parallel sets of MD simulation with different initial velocities were performed. The first two steps included a 50 ps isothermal-isochoric (NVT) simulation followed by a 50 ps isothermal-isobaric (NPT) simulation to allow the solvent molecules to equilibrate. In both simulations, the heavy atoms of the complex were restrained by a harmonic potential with a force constant of 1,000 kJ × mol^{-1} × nm^{-2}. Two subsequent steps without restraints, including a 100 ps NVT simulation and a 100 ps NPT simulation, were performed to equilibrate the entire system. The temperature was kept at 300 K in all NVT and NPT simulations using the v-rescale thermostat with a time coupling constant of 0.1 ps. A pressure of 1 bar was employed in all NPT simulations using the Parrinello-Rahman barostat with a time coupling constant of 2.0 ps and isothermal compressibility of 4.5 × 10^{-5} bar^{-1}. The LINCS constraint algorithm was applied to all bonds during equilibrations. Periodic boundary conditions were used in all directions of the unit cell. A cutoff of 1.0 nm was imposed for both Lennard-Jones and electrostatic interactions. The particle mesh Ewald approach treated the electrostatic interaction beyond the cutoff distance with a Fourier spacing of 0.12 nm and cubic interpolation. A long-range dispersion correction for energy and pressure was applied to account for the 1.0 nm cutoff of the Lennard-Jones interactions. The dynamic equations were integrated using the leapfrog algorithm, with a time step of 2 fs. Then, the production simulation was performed in the NPT ensemble for 100 ns. MD parameters for production simulations were the same as the ones described in NPT equilibrations, except that the LINCS constraint algorithm was now applied to only bonds involving

hydrogens.

Root-mean-square deviation (RMSD) and root-mean-square fluctuation (RMSF) calculations. We used the 50–100 ns segment of the trajectories to calculate RMSD and RMSF. RMSD was computed using the carbonyl carbon atom of the N-fatty acid, the backbone atoms (N, Cα, and C) of residues 2–6 and 8–11, and the Cβ and Nγ atoms of the second residue, Dap2. Residues Ser1 and Ser7 were excluded from the RMSD calculations because they form bonds with PBA, and our focus was on the deviation of the remaining peptide from the X-ray crystal structure.[1] RMSF was calculated using the Cα atoms of residues 1–11.

Figure S1. ITC traces of C10P titration into **B1**/PBA/Ca^{2+}

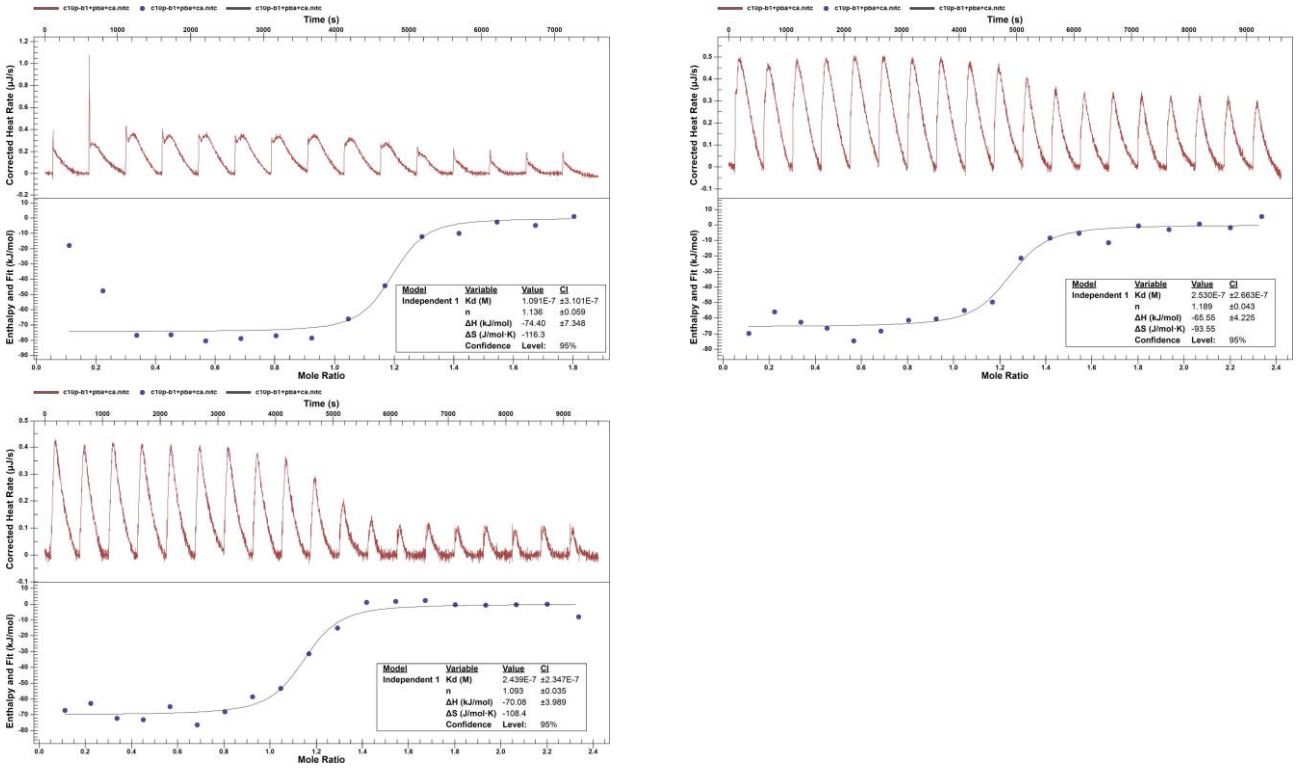

Figure S2. ITC traces of C10P titration into **B1**/PBA

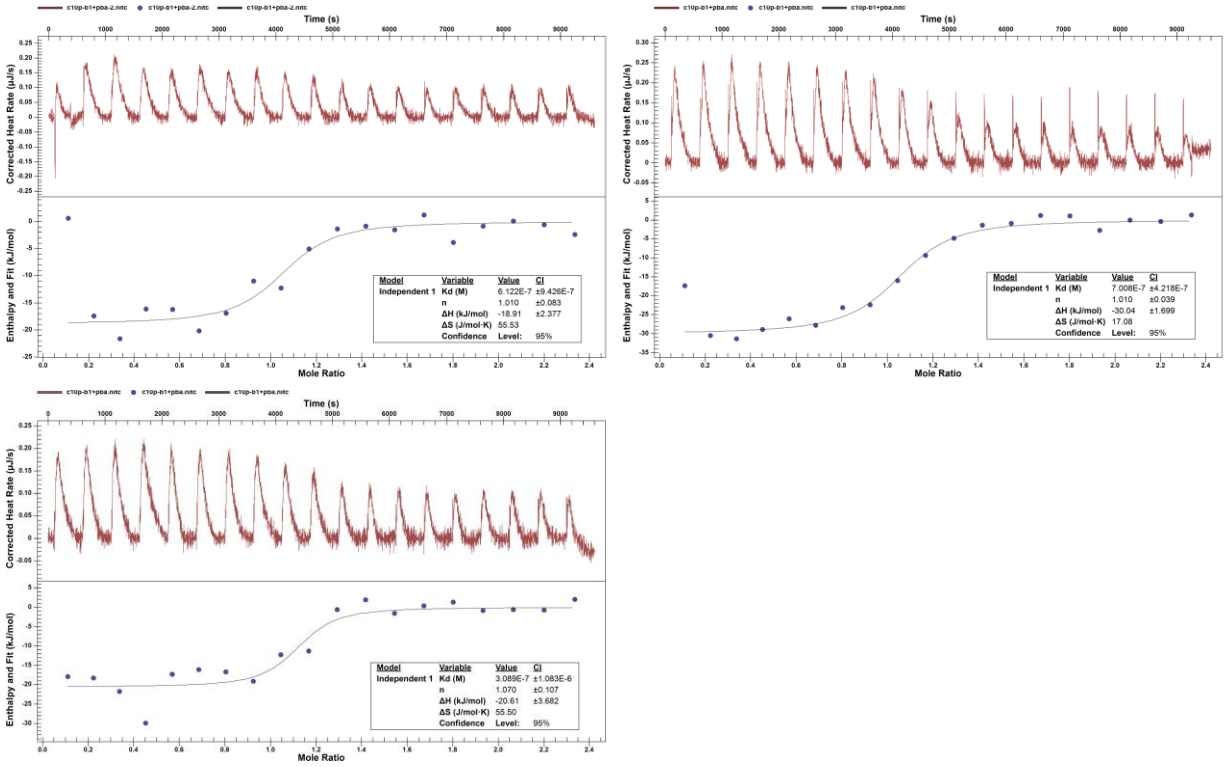

Figure S3. ITC traces of C10P titration into **B1**/Ca^{2+}

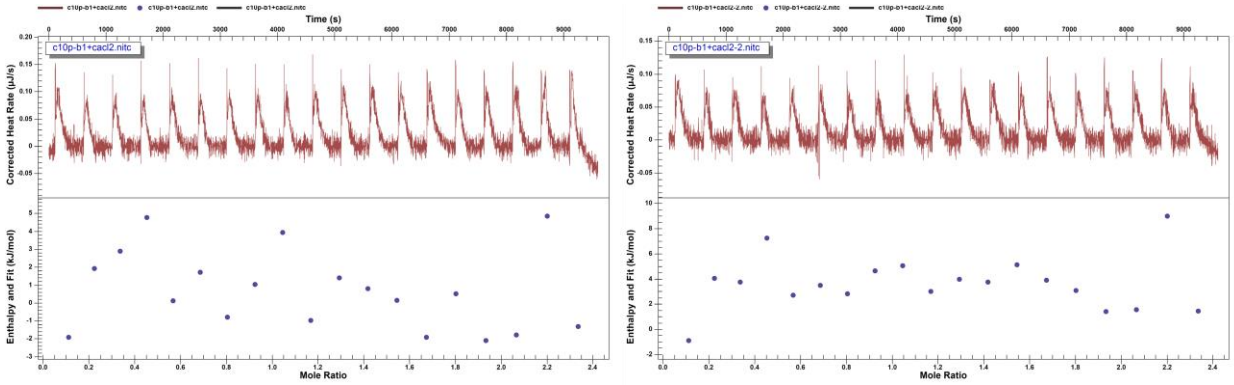

Figure S4. ITC traces of C10P titration into **B1**

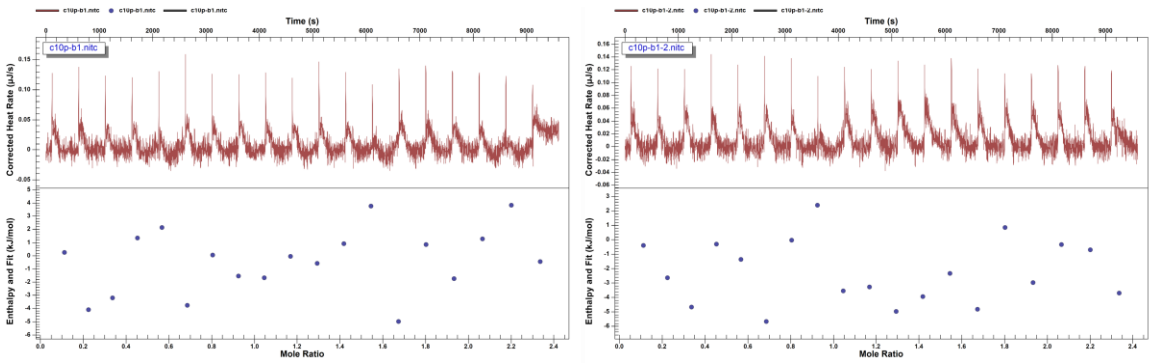

Figure S5. ITC traces of PBA titration into **B1**

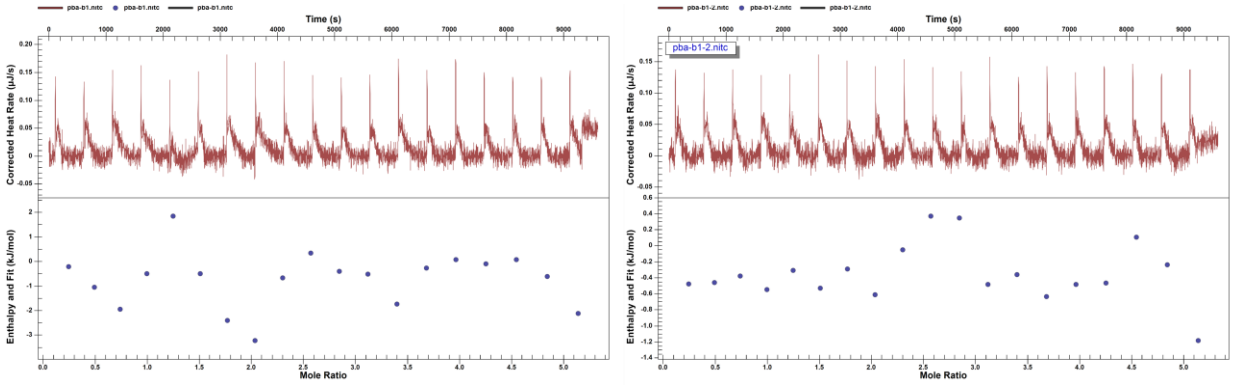

Figure S6. ITC traces of C10P titration into **S1**/Ca^{2+} titrated by **C10P**

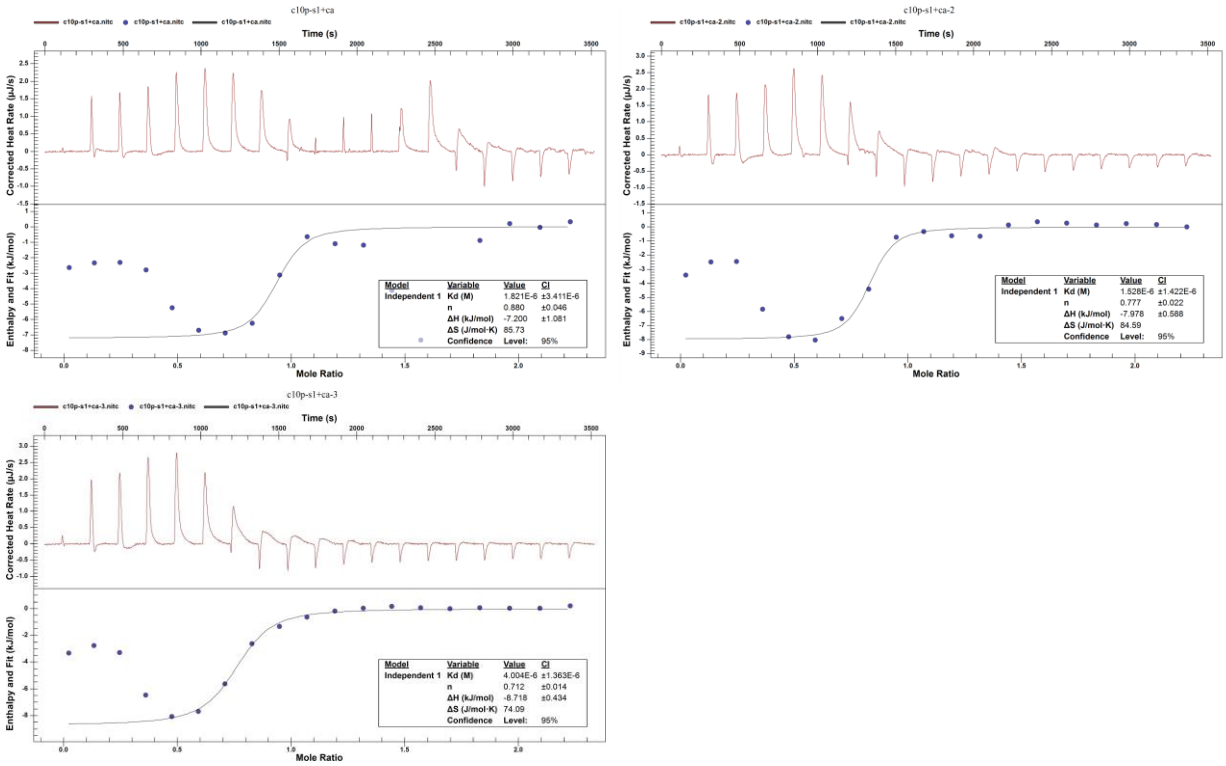

Figure S7. ITC traces of C10P titration into **S1**

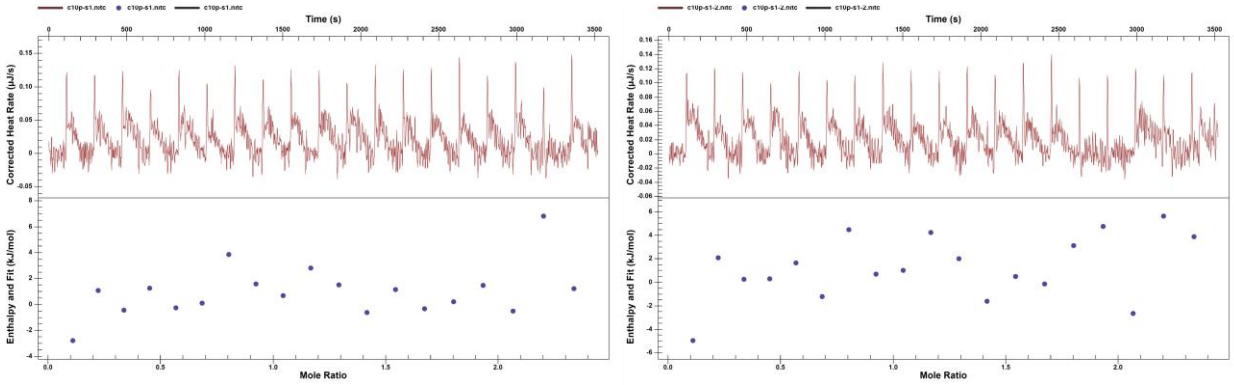

Figure S8. ITC traces of Ca(II) titration into **S1**

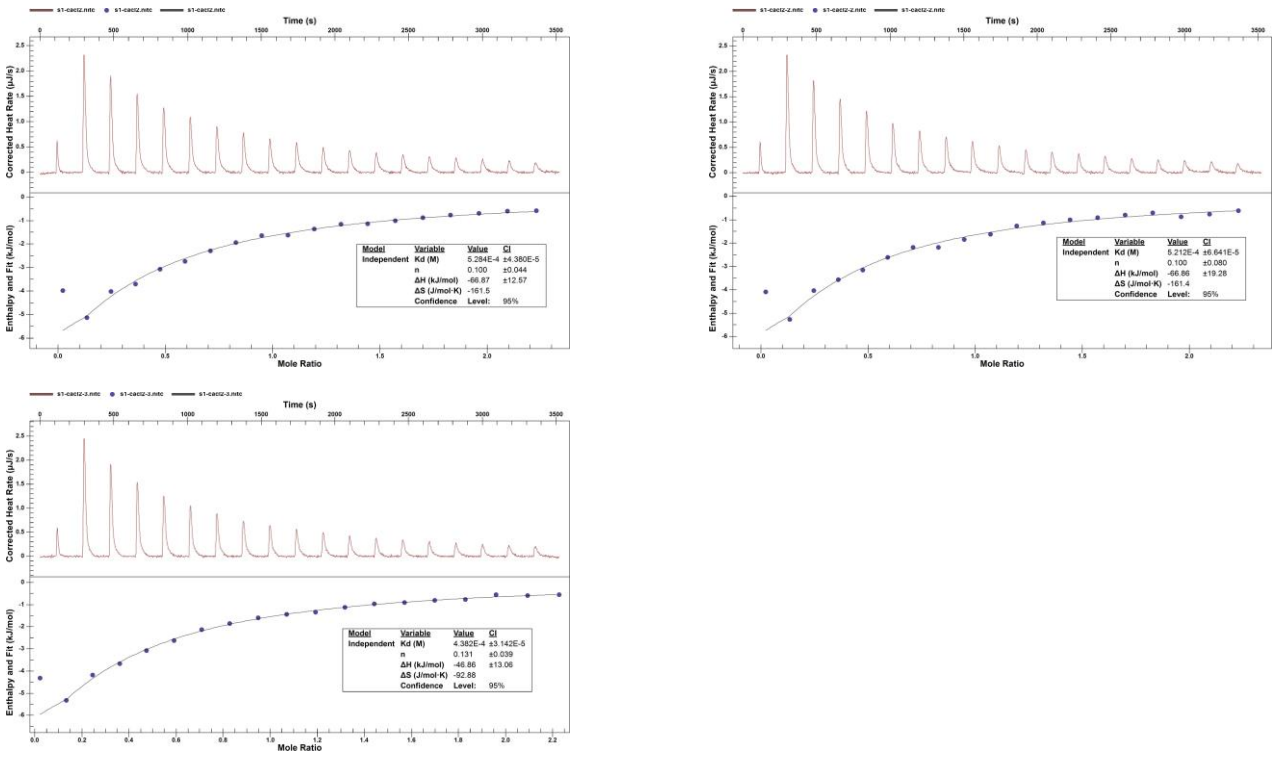

Figure S9. ^{19}F NMR spectra of FPBA with and without glucose

The top trace is ^{19}F NMR (400 MHz) spectrum of a saturated solution of FPBA in 150 mM NaCl and 20 mM HEPES at pH 7.4 with 10% (v/v) D_2O. After the addition of glucose (1 M), ^{19}F spectrum was again acquired and shown as the bottom trace. The peaks at δ –110 and –118 ppm correspond to FPBA and the FPBA/glucose complex, respectively.

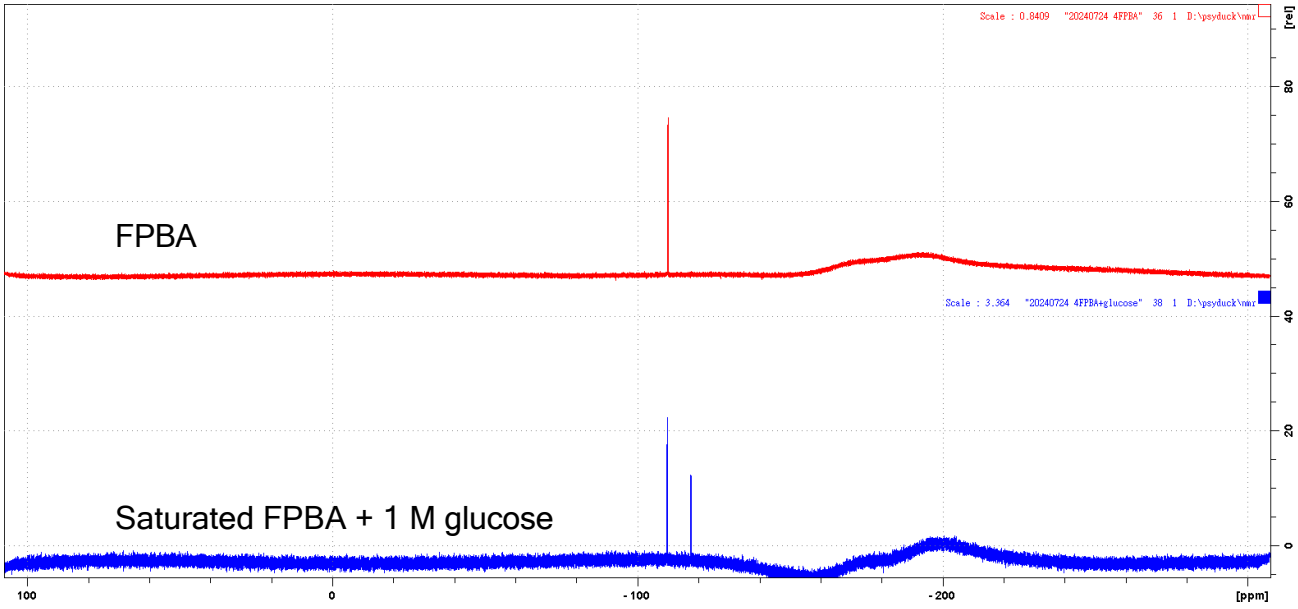

Figure S10. ITC traces of C10P titration into PBA

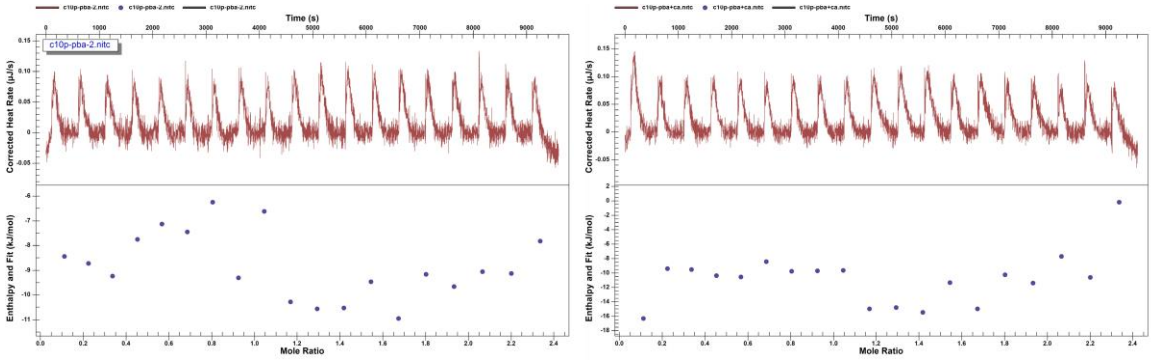

Figure S11. Structural ensembles of various **B1**/PBA/C10P complexes by MD simulation

The **B1**/PBA/C10P ternary complex contains three boron–oxygen (B–O) bonds, wherein the boron in PBA is connected to the oxyanion of C10P and the side-chain OH of Ser7 and Ser1. The B–O bonds were removed one at a time to generate three new **B1**/PBA/C10P complexes that served as the starting point for MD simulation. Shown below are the structural ensembles of **a)** the complex with all B–O bonds intact and **b–d)** three complexes each with one B–O bond removed. The simulated structures are aligned to the LspC/Ca(II)/C10P X-ray crystal structure based on their amino acid backbone atoms.

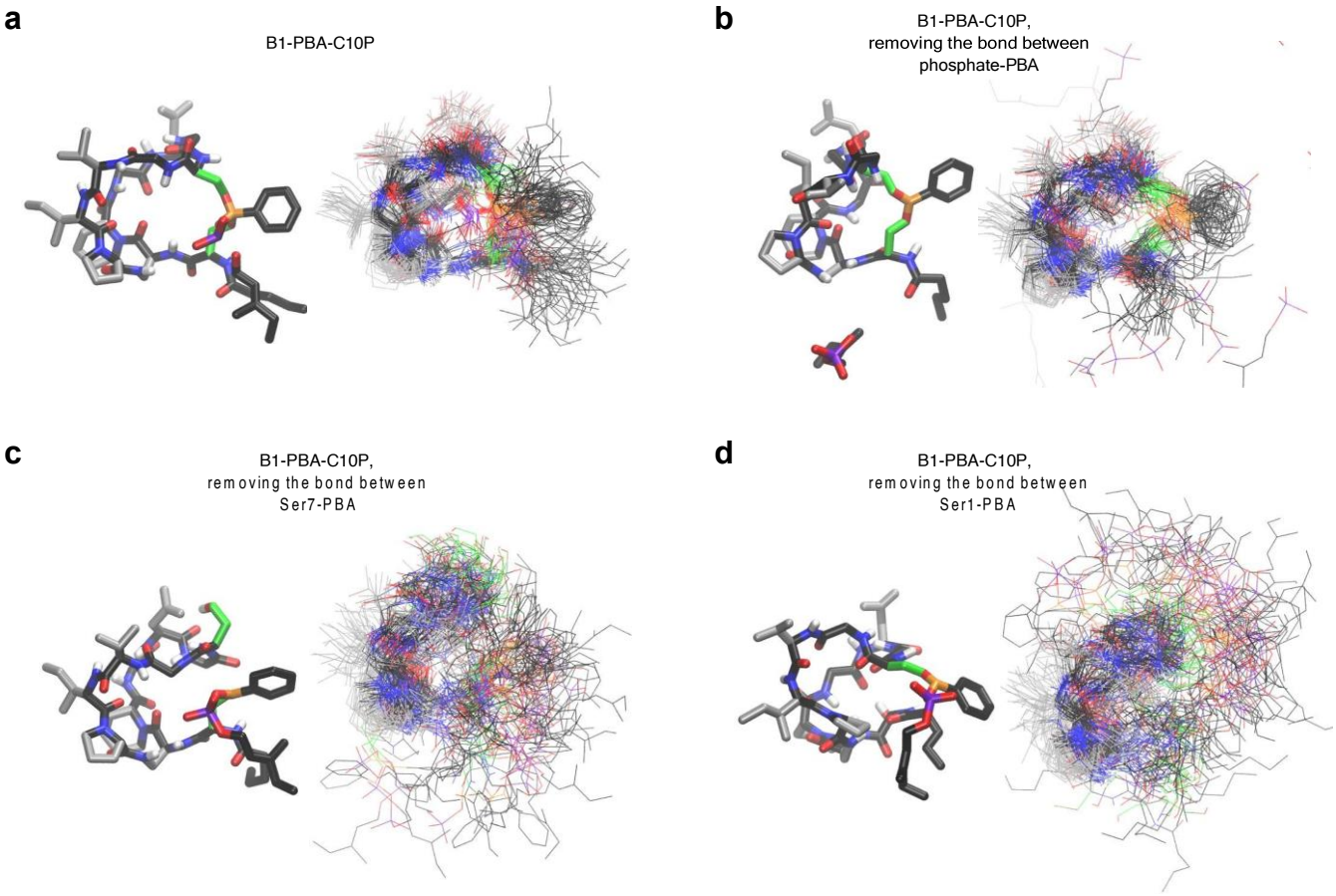

Figure S12. RMSD and RMSF of various **B1**/PBA/C10P complexes by MD simulation

RMSD (column **a**) and RMSF (column **b**) of various **B1**/PBA/C10P complexes (see description in the main text and Figure S10). From top to bottom are the complex with all B–O bonds intact, the analogous complexes with the C10P (phosphate)–PBA, Ser7–PBA, and Ser1–PBA bond removed, respectively.

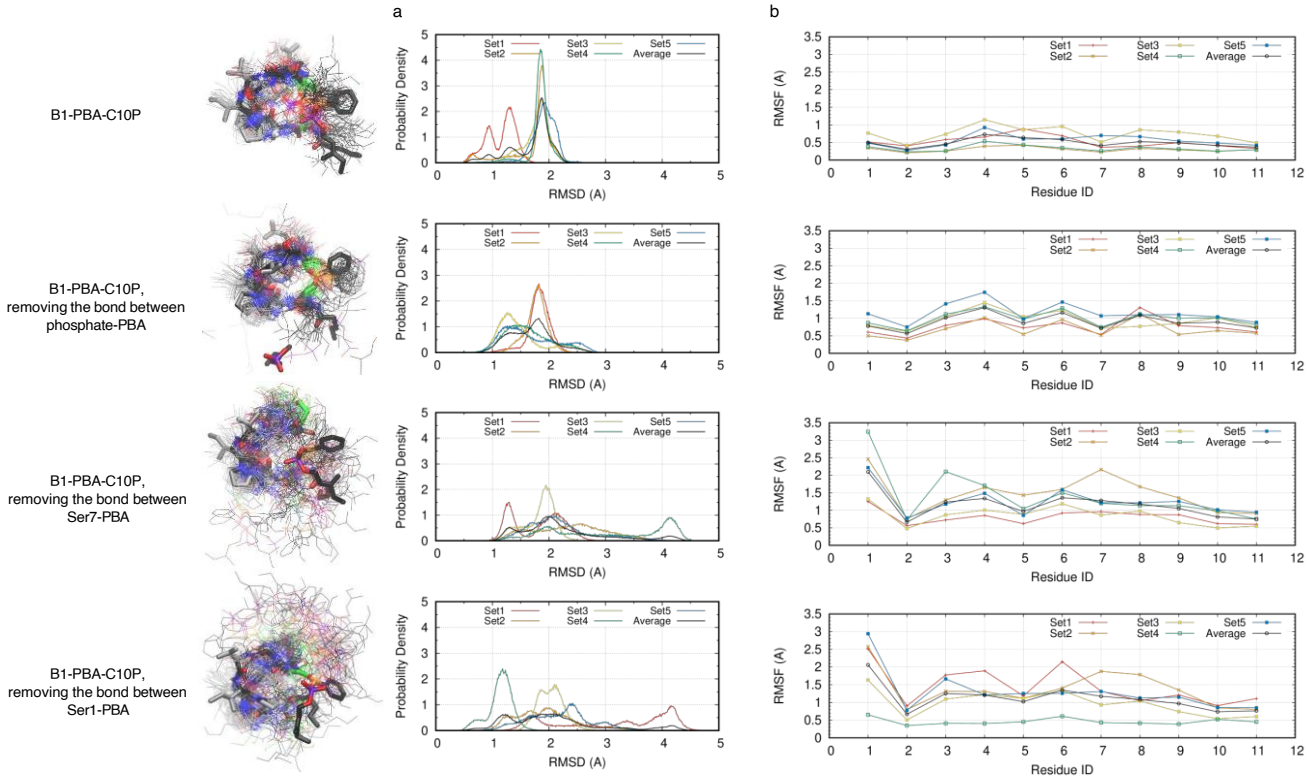

Table S1. Reported boronic acid / diol condensation rate constants[7, 8]

Boronic acid	Alcohol	K_{eq}	$k_{obs,f}$ (s^{-1})	$k_{obs,r}$ (s^{-1})	Note
$PhB(OH)_2$	Neopentylglycol	0.577	0.0473	0.082	Ref.8 [a]
	Trimethylethane	1.389	0.1100	0.0792	
	Sorbitol	7.4	0.23	0.031	
	cis-1,2-cyclopentanediol	15	0.0216	0.0014	
$3\text{-}PyB(OH)_2$	Tiron	3.69	2.50×10^4	6.78×10^3	Ref.9 [b]
	Tiron-H	1.06	4.35×10^3	4.10×10^3	
$3\text{-}NO_2PhB(OH)_2$	Ethylene glycol	2.35×10^{-7}	1.01×10^4	4.30×10^{10}	
	Propylene glycol	5.55×10^{-7}	5.77×10^3	1.04×10^{10}	
$3\text{-}FPhB(OH)_2$	Propylene glycol	1.29×10^{-7}	4.63×10^3	3.58×10^{10}	
$PhB(OH)_2$	Propylene glycol	1.34×10^{-8}	7.49×10^2	5.57×10^{10}	

[a] Experiments performed in d_6 acetone/D_2O = 1.2:1 at 25 °C

[b] Experiments performed in CAPS buffer or self-buffered at 25 °C

References

1) Chiou, S.-L.; Chen, Y.-J.; Lee, C.-T.; Ho, M. N.; Miao, J.; Kuo, P.-C.; Hsu, C.-C.; Lin, Y.-S.; Chu, J. A Boron-Dependent Antibiotic Derived from a Calcium-Dependent Antibiotic. *Angew. Chem. Int. Ed.* **2024**, *63*, e202317522.
2) Kleijn, L. H. J.; Vlieg, H. C.; Wood, T. M.; Toraño, J. S.; Janssen, B. J. C.; Martin, N. I. A High-Resolution Crystal Structure that Reveals Molecular Details of Target Recognition by the Calcium-Dependent Lipopeptide Antibiotic Laspartomycin C. *Angew. Chem. Int. Ed.* **2017**, *56*, 16546-16549.
3) *Schrödinger Release 2024-4: Maestro*; Schrödinger, LLC: New York, NY, 2024.
4) Frolov, A. I.; Kiselev, M. G. Prediction of Cosolvent Effect on Solvation Free Energies and Solubilities of Organic Compounds in Supercritical Carbon Dioxide Based on Fully Atomistic Molecular Simulations. *J. Phys. Chem. B* **2014**, *118*, 11769-11780.
5) Abraham, M. J.; Murtola, T.; Schulz, R.; Páll, S.; Smith, J. C.; Hess, B.; Lindahl, E. GROMACS: High Performance Molecular Simulations through Multi-Level Parallelism from Laptops to Supercomputers. *SoftwareX* **2015**, *1-2*, 19-25.
6) Banks, J. L.; Beard, H. S.; Cao, Y.; Cho, A. E.; Damm, W.; Farid, R.; Felts, A. K.; Halgren, T. A.; Mainz, D. T.; Maple, J. R.; et al. Integrated Modeling Program, Applied Chemical Theory (IMPACT). *J. Comput. Chem.* **2005**, *26*, 1752-1780.
7) Jorgensen, W. L.; Chandrasekhar, J.; Madura, J. D.; Impey, R. W.; Klein, M. L. Comparison of Simple Potential Functions for Simulating Liquid Water. *J. Chem. Phys.* **1983,** *79*, 926-935.
8) Kang, B.; Kalow, J. A. Internal and External Catalysis in Boronic Ester Networks. *ACS Macro Letters.* **2022**, 11, 394-401.
9) Watanabe, E.; Miyamoto, C.; Tanaka, A.; Iizuka, K.; Iwatsuki, S.; Inamo, M.; Takagi, H. D.; Ishihara, K. Relative Kinetic Reactivity of Boronic Acid and Boronate Ion Towards Tiron, 2,2'-Biphenol, and Propylene Glycol. *Dalton Trans.* **2013**, *42*, 8446-8453.